SIMULATION OF SEMICONDUCTOR DEVICES AND PROCESSES Vol. 3
Edited by G. Baccarani, M. Rudan - Bologna (Italy) September 26-28, 1988 - Tecnoprint

2D SIMULATION OF DEGENERATE HOT ELECTRON TRANSPORT IN MODFETs INCLUDING DX-CENTER TRAPPING

TAREK SHAWKI*, GEORGES SALMER* and OSMAN EL-SAYED**

* Centre Hyperfréquences et Semiconducteurs
U.A. C.N.R.S. n° 287 - Bât. P4
Université des Sciences et Techniques de Lille Flandres Artois
59655 VILLENEUVE D'ASCQ CEDEX - FRANCE.

** Electronics and Communication Department
Faculty of Engineering - Cairo University - EGYPT.

ABSTRACT

A comprehensive 2D-hydrodynamic-energy model that is capable of describing nonstationary electron dynamics and non isothermal transport within submicron MODFETs is presented. The model accounts for carrier degeneracy, deep-donor levels and conduction outside the quantum well. It is exploited systematically to predict the small and transient large signal performance of conventional .3 μm gate $Al_{.3}Ga_{.7}As$/GaAs MODFETs operating at room temperature. The model is so informative that it highlights the main physical phenomena that occur in these devices and we are first to report the occurance of a local longitudinal field inversion region at the gate entrance of the channel. Moreover, we present two original techniques developed to overcome the complexity of solving the model coupled non linear partial differential equations (PDEs). The first concerns trapping mechanisms and the 2nd is devoted to the energy conservation equation.

1. INTRODUCTION

Existing heterostructure-device models may be divided into two broad classes :

(i) One-dimensional analytical and numerical models that suffer from a large number of unsuited simplifying assumptions.

(ii) Two-dimensional models which may be further devided into either :

- sophisticated Monte Carlo (MC) models which, while quasi exact, suffer from the large-involved computational efforts and the inability to handle transient and dynamic behavior, or ;
- hydrodynamic models which are based on a set of conservation equations and may be further subdevided into :

- local models, (Lundstrom, 1983 ; Loret, 1987) which sacrifice hot electron effects for the sake of simplicity and,
- temperature or energy models, like the one being presented, which on the time being possess the best price/accuracy trade off. The first such model was introduced by Widiger et al (1984). They included quantum effects by simulating the lowest quantum subband but, however, they neglected the AlGaAs so that trapping, real space transfer and parasitic MESFET effects did not play a role.

This paper is organized so as the fulfill the following objectives, presented thereafter in order :

(i) To elaborate a reliable physical model that is capable of describing the different physical phenomena involved in electron transport within submicron MODFETs. This includes non-stationary electron dynamics and non-isothermal transport, conduction outside the quantum well, real space transfer, electron degeneracy and electron trapping mechanisms responsible for the observed different anomalies at cryogenic temperatures.

(ii) To develop the numerical methods necessary for solving the model equations as accurate as possible and with the smallest computational efforts. This is based on fully implicit and semi-implicit decoupling techniques over non uniform-mesh recessed as well as planar structures.

(iii) To exploit the model systematically to highlight the physical phenomena governing the device performance and to predict its behavior under dynamic and transient conditions.

2. MODEL DESCRIPTION

Generally, the model equations comprise pure-transport as well as collision terms. Whereas collision terms are formulated pheneomenologically by appropriate relaxation times, transport terms are derived by taking the first 3 moments of Boltzmann transport equation (Marschak, 1984) :

$$(1) \qquad \frac{df}{dt} = \frac{\partial f}{\partial t} + \underline{v}\cdot\underline{\nabla}_r f - \frac{1}{\hbar}(\underline{\nabla} E_c + \underline{\nabla} W)\cdot\underline{\nabla}_k f = \left(\frac{\partial f}{\partial t}\right)_c$$

to arrive at 3 conservation equations for particle, momentum and energy respecitvely. The assumptions usually made are primarly those made by Blotekjaer (1972). The most relevent is that the relaxation time for equivalent valley scattering is shorter than all other relevent time constants so that one needs consider only 3-isotropic valleys (Γ, L and X), the distribution function in each of which is fully specified by its local parameters n_i, v_i and T_i.

The transport problem, so far, is too complicated to be of any practical use and is simplified considerably if instead of treating 3 distinct electron gases, we consider an equivalent single electron gas whose parameters are the weighted averages of the parameters of the constituting gases. Adding Poisson's equation, it

can be shown that carrier transport is governed by the following set of equations where we used the notation of positive electrons :

(2) $$\frac{\partial n}{\partial t} = -\underline{\nabla}\cdot n\,\underline{v} + G_n - R_n$$

(3) $$\left|\frac{\partial}{\partial t}[n m^*(\xi) v_x] + \underline{\nabla}\cdot n m^*(\xi) v_x \underline{v}\right| \frac{1}{q} + n\frac{v_x}{\mu(\xi)} =$$

$$-n\left|\underline{\nabla}(\phi - \chi) + \frac{\underline{\nabla}(n k_B T_e(\xi))}{n} - W\,\underline{\nabla}\ell n\left[m^*(\xi)\right]\right|\cdot \underline{a}_x$$

(4) $$\frac{\partial \xi}{\partial t} = -\underline{v}\cdot\underline{\nabla}(\phi - \chi + \xi) - \frac{\underline{\nabla}\cdot(n k_B T_e(\xi)\,\underline{v})}{n} - \frac{\xi - \frac{3}{2} k_B T_o}{\tau_\xi(\xi)}$$

(5) $$\underline{\nabla}\cdot(\varepsilon\,\underline{\nabla}\,\phi) = -q\,(n - N_D^+)$$

(6) $$N_D^+ = \frac{N_D}{1 + 2e^{(E_{fn} - E_d)/k_B T_e(\xi)}} \quad \text{where}$$

χ, W, ξ, T_e and T_o are the electron affinity, the average kinitic energy, the total average energy, the equivalent electronic temperature and the lattice temperature respectively. The other terms have their usual meaning. Similar to (3), two other equations exist in the other two directions. The physical parameters are all taken to be dependent on the average total energy which are then obtain from steady state Monte-Carlo simulations.

2.1. SIMULATION OF CARRIER DEGENERARY

The simulation of transport of hot carriers that obey Fermi-Dirac statistics is a rather difficult task. Recently, Azoff (1987) proposed a method to include these effects in which the "electronic temperature"is not used. The "electronic temperature" is however useful from the simulation point of view since if may permit us to relate the quasi Fermi level to the electron concentration under non isothermal transport simply by assuming that the probability of finding an electron at a certain energy in the conduction band is a function of the equivalent electronic-temperature rather than the lattice one. To retain the electronic temperature, we introduced the following definition :

(7) $$\xi = 1/2\, m^*(\xi)\, v^2 + 3/2\, k_B T_e(\xi)\, \gamma_c + U_p \quad \text{where}$$

(8) $$\gamma_c = \frac{F_{3/2}(\eta_c)}{F_{1/2}(\eta_c)} \quad \text{with} \quad \eta_c = \frac{E_{fn} - E_c}{k_B T_e}$$

(9) $$n = 2\left(\frac{m^*(\xi)k_B T_e(\xi)}{2\Pi\hbar^2}\right)^{3/2}\left|F_{1/2}(\eta_c) + \frac{15\,\alpha k_B T_e(\xi)}{4\varepsilon_i} F_{3/2}(\eta_c)\right|$$

where γ_c, defined as above, is introduced by Azoff (1986). The electron concentration n accounts for the non parabolicity of the GaAs conduction band. Multiplying T_e and T_o in (3) & (4) by γ_c, we arrive at the system of equations corresponding to the degenerate limit.

3. THE NUMERICAL SCHEME

The discretization in space is carried out using Finite-Difference. The mesh is obviously non uniform so that in the direction perpendicular to the heterointerface, the most crucial, it starts by a 20 Å size in the 2DEG channel. It then increases progressively into the AlGaAs as well as the GaAs keeping the ratio between 2 successive meshes always less than 1.15.

The time discretization is accomplished using adoptive time steps that very between $.05\times10^{-14}$ and $.25\times10^{-14}$ sec depending on the values of the displacement currents. Our variables are chosen to be the total electronic energy ξ, the electrostatic potential ϕ measured from the conduction band Γ-minimum at the source side and the electron concentration n rather than the quasi-Fermi level.

Semi and fully implicit decoupling techniques are employed and in both of which the continuity and energy equation are solved self consistently using the iterative Newton SOR method to update n^k, corresponding to the k^{th} Newton step of the i^{th} time step, which is then substituted in Poisson's equation to find ϕ^k.

The latter equation is solved, however, exactly using an elaborated Cholesky LLT decomposition technique developed by Ibrahim (1983) and termed the Matrix-Double-Sweep (MDS) method. Obviously, then, the introduction of an adaptive mesh refinement will be at the expense of revaluating the decomposition matrices which is a relatively slow operation and is performed only once by the preprocessor. To gain in CPU time, it is hence essential to optimize the process which thus opens the door for further research.

3.1. TREATMENT OF DEEP LEVELS

The DX-centres are simulated as presented in (6) by assuming the presence of a single equivalent deep donor level situted at 160 mev below the L valley (Theis, 1986). This complicates the situation as it not only makes the R.H.S. of (5) a nonlinear function of the electrostatic potential, but it also introduces generation-recombination terms in the continuity equation (2) to account for the trap capture-emission rates. In that respect, an original method has been developed by the authors in order to account for these effects. This method while rigorous, is of minor cost. The essence of this method is the following. Assuming the (G_n-R_n) terms in equation (2) to be only dependent on the density of the ionized donors, the continuity equation then reads :

(10) $$\frac{\partial n}{\partial t} = -\underline{\nabla}\cdot n\underline{v} + \left(\frac{\partial N_D^+}{\partial t}\right) \qquad \text{where}$$

(11) $$N_D^+ = \frac{N_D}{1 + 2e^{(E_{fn} - E_d)/k_B T_e(\xi)}} \triangleq$$

$$\frac{N_D}{1 + 2e^{(E_{dd}/k_B T_e)} e^{\eta_c}} \triangleq \frac{N_D}{1 + ge^{\eta_c}}$$

A time differentian of this equation then gives :

(12) $$\frac{\partial N_D^+}{\partial t} = \frac{-N_D\left(ge^{\eta_c}\frac{\partial \eta_c}{\partial n}\right)}{\left(1 + ge^{\eta_c}\right)^2}\frac{\partial n}{\partial t} \triangleq -f^+(n)\frac{\partial n}{\partial t}$$

The term representing $(\partial\eta_c/\partial n)$ in the last equation can, in principle, be derived from equation (8). It can be easily shown that, if Maxwell-Boltzman statistics hold, it takes the following form :

(13) $$f^+(n) = \frac{g N_{cj} N_D}{\left(N_{cj} + n g\right)^2}$$

where N_{cj} is the joint density of states. Substituling in (12) gives the following form of the current continuity equation :

(14) $$\frac{\partial n}{\partial t}\left[1 + f^+(n)\right] = -\underline{\nabla}\cdot n\underline{v}$$

which can be easily solved using Newton SOR methods. Substituling the resulting value of n^k obtained at the kth Newton iteration in (11), we obtain $N_D{}^{+k}$ which is required to solve Poissons equation for Φ^k.

3.2. THE ENERGY EQUATION

The discretization of this equation is so crucial that most of the authors working on temperature or energy models admit that it always represents the most complicated and critical step and is resposible for the solution sensitivity as well as the successive numerical instabilities if present. This is clear since the investigation of (3) reveals that even semi-implicitly, this equation rests a nonlinear PDE with variable coefficients.

In order to overcome this, we have developed a numerical technique, the essence of which is to linearize (3) benefiting from the available steady-state MC results. The details follow. Consider

the non-degenerate form of the energy equation. Replacing ξ-ξ_o by ξ, then (3) reads :

$$\frac{\partial \xi}{\partial t} = -\underline{v}\cdot\underline{\nabla}(\phi - \chi + \xi) - \frac{\underline{\nabla}\cdot[n T_e(\xi)\,\underline{v}(\xi)]}{n} - \frac{\xi}{\tau_\xi(\xi)} \tag{15}$$

which, once discretized in time and Taylor expanded gives :

$$\frac{\delta\xi^{k+1}}{\delta t} \triangleq F_\xi(n^{k+1}, \phi^{k+1}, \xi^{k+1}) = \tag{16}$$

$$F_\xi(n^k, \phi^k, \xi^k) + \frac{\partial F_\xi}{\partial n}\bigg|_k \delta n + \frac{\partial F_\xi}{\partial \phi}\bigg|_k \delta\phi + \frac{\partial F_\xi}{\partial \xi}\bigg|_k \delta\xi \tag{17}$$

The evaluation of the 2nd and 3rd terms of the RHS is straighforwad so that we will restrict our attention to the last one. This reads :

$$\left(\frac{\partial F_\xi}{\partial \xi}\right)_k \delta\xi = -\underline{v}\cdot\underline{\nabla}\,\delta\xi - (1/n)\,\underline{\nabla}\cdot\Big[n T_e'(\xi)^k\,\delta\xi\,\underline{v}(\xi^k) \tag{18}$$

$$+ n T_e(\xi^k)\left(\frac{\partial \underline{v}}{\partial \xi}\right)\delta\xi\Big] - \frac{\tau_\xi\,\delta\xi - \xi_k\,\tau_\xi'(\xi^k)\,\delta\xi}{\tau_\xi^{\,2}(\xi^k)}$$

where [$'(\xi^k)$]denotes the derivative w.r.t. energy evaluated at ξ^k.

$$v' \triangleq \left(\frac{\partial \underline{v}(\xi)}{\partial \xi}\right)_k \delta\xi = -\mu'(\xi)\,\delta\xi\left(\frac{\underline{v}}{\mu(\xi)}\right)_k \tag{19}$$

$$- \mu_k(\xi^k)\left\{\frac{\underline{\nabla} n T_e'\,\delta\xi}{n} - W^k\,\underline{\nabla}\ln m'^*\,\delta\xi - (\underline{\nabla}\ln m^{*k})\left(\frac{\partial W}{\delta\xi}\right)_k \delta\xi\right|$$

$$\tau_\xi' \triangleq \left(\frac{\partial \tau_\xi}{\partial \xi}\right)_k, T_e' \triangleq \left(\frac{\partial T_e}{\partial \xi}\right)_k \text{ and } \mu'(\xi) \triangleq \left(\frac{\partial \mu}{\partial \xi}\right)_k \tag{20}$$

The dynamic parameters as well as their derivatives being obtained from steady state MC simulation, the solution is thus complete.

4. RESULTS AND COMMENTS

The simulated structure is the conventional .3μ gate one presented in Fig. 1. It consists of a 360 Å heavily doped $Al_{.3}Ga_{.7}As$ layer (doping = 10^{18} cm^{-3}) followed by a 40 Å $Al_{.3}$ $Ga_{.7}$ As undoped spacer grown on an undoped GaAs buffer. The variation in composition is assumed to occur over a distance of about 20 ~ 40Å, and the conduction band discontinuity is taken to be .23 ev. The gate built in voltage is taken to be .8v.

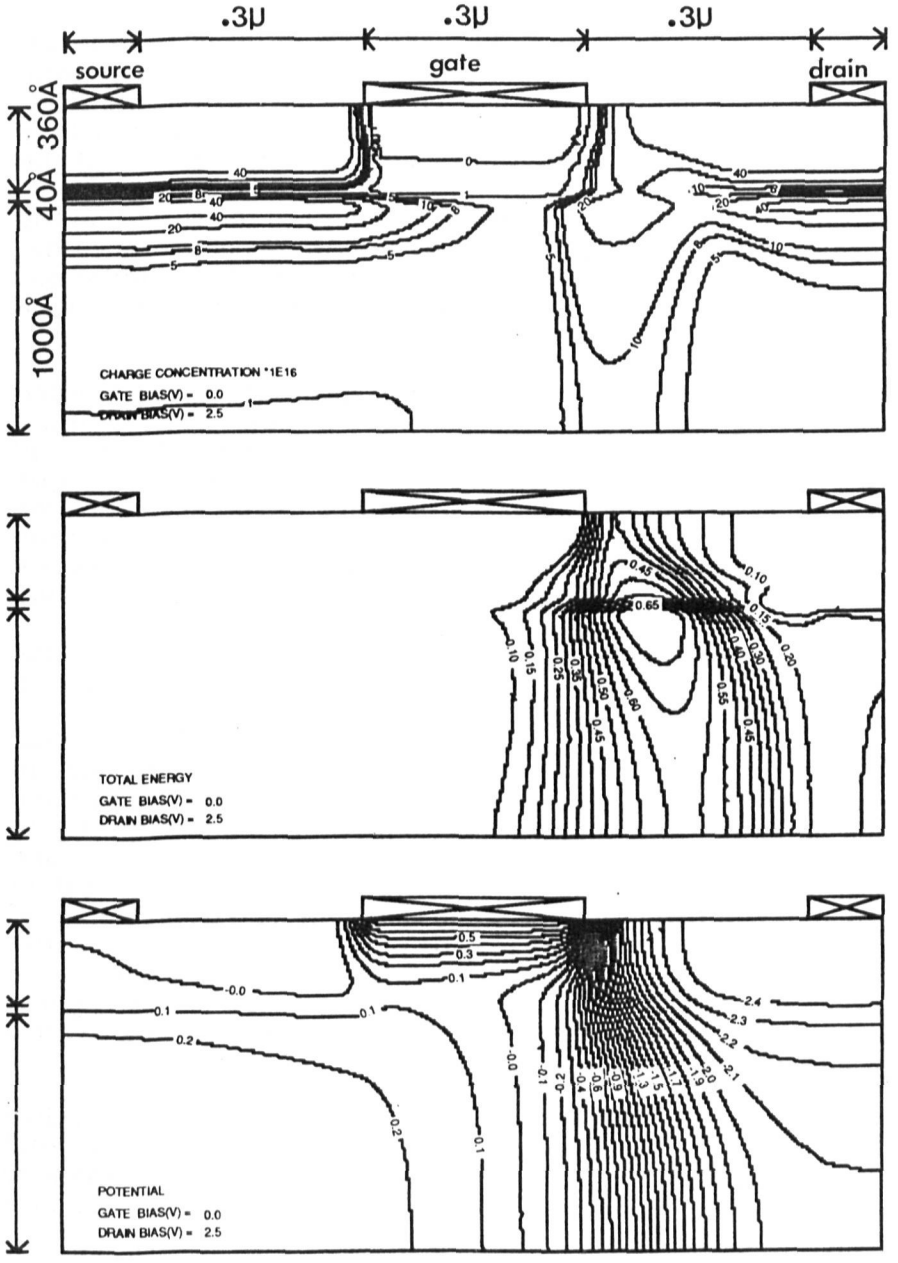

Fig. 1.a) A typical distribution of the electron density $*10^{16}$ demonstrating injection effects at the gate entrance & exit of the channel. b) Isolines of the total average electron energy illustrating the formation of a stationary high field domain at the gate exit of the channel. c) The corresponding equi-potential contours illustrate that the 2DEG is submitted to a negative potential up to the middle of the gate.

Fig. 1 illustrates a sample isolines for the electron concentration, total energy and potential respectively, from which to be observed that a stationary high field domain whose total energy peaks at about .7 ev is formed at the gate-exit of the 2DEG channel. Fig. 1.c) demontrates that the 2DEG submitted to a negative potential from the source side up to the middle of the gate. This results from the 2 dimensional nature of Poisson's equation. It is to be expected, then, that most of the current in the source-gate region will be carried by the AlGaAs electrons rather than the 2DEG. A result which is confirmed by MC simulations (Thobel, 1988). It is therefore essential to optimize the source resistance as far as possible.

Furthermore, the electronic charge distribution, represented in Fig. 1a), demonstrates two important injection effects occuring at the gate entrance and exit of the channel respectively. This can be also seen from Fig. 3.b) which represents the total GaAs charge as a function of distance and bias. The former occurs in conjunction with the appearance of a local channel-longitudinal field inversion (Fig. 2.a)) that grows in absolute magnitude with the gate reverse bias to reach 28 kv/cm at a gate bias of -.4v. This provokes two effects :

First a local channel depletion region that extends to join the gate one is generated so that carriers are forced to be injected onto the GaAs buffer layer.

Second the electric field in the immediate vicinity grows up, quickly (100 kv/cm at .4v and 170 kv/cm at -.4v of gate bias) to counteract this inversion or equivalently to absorb the applied drain voltage. Consequently, electrons will be heated quickly so that they undergo a premature transfer to the satellite valleys and thus their average velocity peaks at the middle of the gate rather than at its exit (Fig. 2.c)). The stationary high field domain formed at the drain side of the gate may be pinned there by virtue of this local field inversion layer. This contrasts the usual picture in MESFET simulators (El-Sayed, 1987) where, once a positive going drain pulse is applied, one observes a traveling wave domain which once discharged reforms at the gate exit.

Electrons, thus, become hot during the main part of their drift underneath the gate such that, at the gate exit, their average total energy exceeds twice the barrier height. As a result, the probability of their scattering to the higher quantum subbands and furthermore to the 3D systems increases.

Although this does not implicitly means that in aquiring energy exceeding the barrier height, electrons become 3D, however, MC simulations affirmed this transfer (Ravaiolli, 1986). Electrons that leave the 2D system recover their lost degree of freedom and are thus able to move in the direction perpendicular to the heterointerface.

These electrons, on their way to reduce their energy will diffuse either to the adjacent AlGaAs layer, thus, performing a

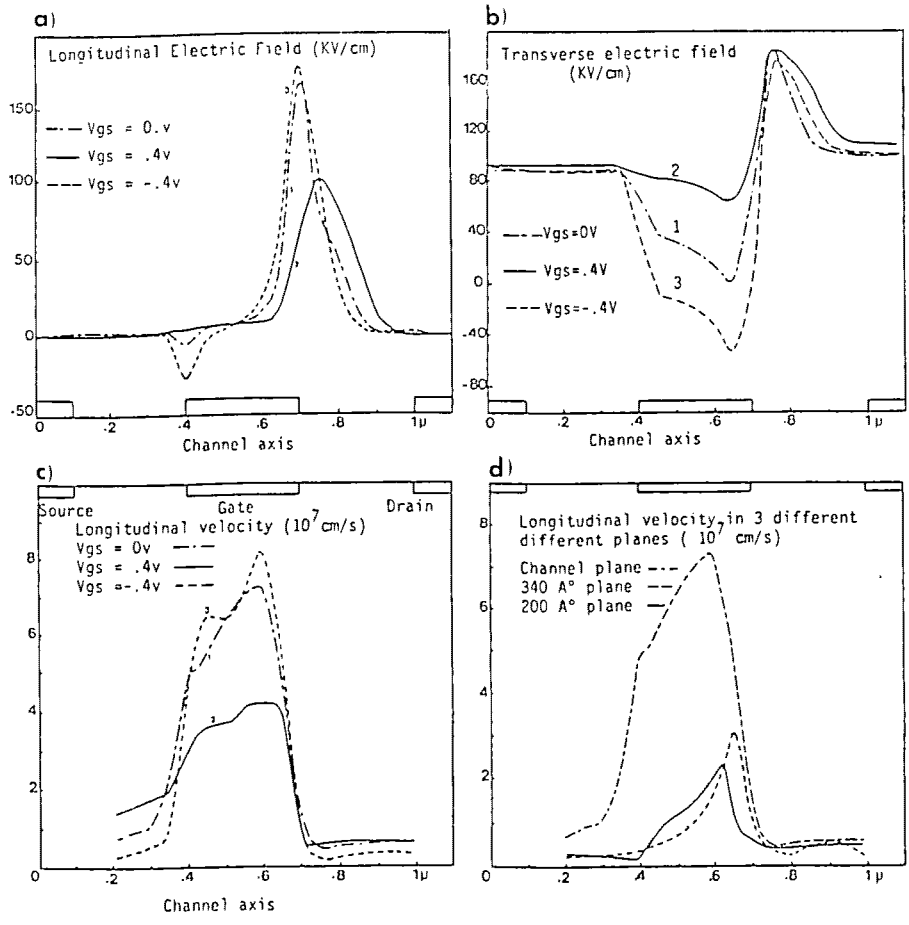

Fig. 2.a) Channel longitudinal field(kV/cm) distribution for different gate voltages and for a typical drain bias of 2v. b) Channel transverse field (kV/cm) distribution for the same conditions as above. c) Corresponding channel longitudinal velocity (*10^7 cm/sec). d) Longitudinal velocity distribution in 3 different planes; in the channel, just before the spacer, and 200A° below the gate. The corresponding gate & drain voltages are 0V & 2V respectively.

back injection to the real space or to the GaAs buffer layer. This is assessed by Fig. 2.b) which demonstrates a somewhat constant value of the transverse field of about (190 kv/cm) all over the voltage range of interest.

In a recent paper (Shawki, 1987), we have demonstrated that the first effect, the more important, is only detrimental to device

performance on the presence of traps. This is expected if we admit that electrons subject to real space transfer will start making their excursion by moving from the GaAs satellite valley to the AlGaAs L and X valley where the DX-center trap associated with the L valley is waiting for them. Other wise these electron will be scattered to the AlGaAs Γ valley so as to keep the statistical balance. Electrons, becoming cold on crossing the junction, will benifit from the AlGaAs low-field mobility which in terms of electron velocity means that they will travel at velocities more or less comparable with those of hot electrons in the GaAs gate-drain region i.e. the saturation velocity(Fig. 2.d)).

On the other hand, electrons released from the quantum subbands and injected into the substrate will be out of the control of gate voltage and hence the transconductance will decrease dramatically if it were not for important increase of overshoot effects (20 % from Fig. 2.c)) with the gate reverse bias.

It is well known that, parasitic MESFET effects deteriorates the device performance drastically because of the inferior properties of the heavily doped AlGaAs layer. Varying the gate voltage around the point where the AlGaAs starts to be undepleted merely controls the free electrons present in the AlGaAs layer that undergo scattering due to ionized impurities and hence does not show significant overshoot effects. This can be depicted from Fig. 4.a) which demonstrates a steep fall in the transconductance and cut-off frequency with moderate forward bias. This deterious effect mainly takes place when the 2DEG saturates.

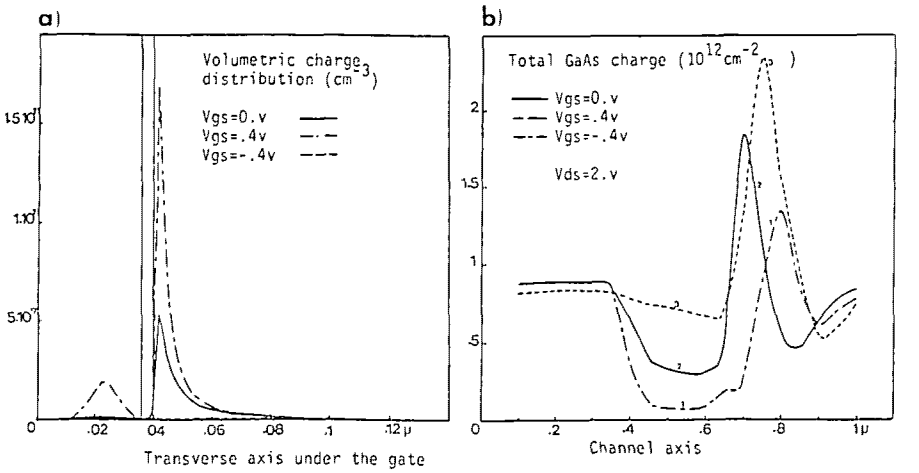

Fig. 3.a) Total GaAs charge ($*10^{12}$ cm^{-2}) for different gate voltages. The drain bias is 2V. b) Euilibrium volumetric charge distribution under the gate for different gate voltages as above.

Fig. 3.a) illustrates the volumetric charge distribution under the gate for different bias conditions. It is interesting to note that, the gate controls the AlGaAs and the GaAs electrons simultaneously so that the gate capacitance will increase steadly as depicted in Fig. 4.a).

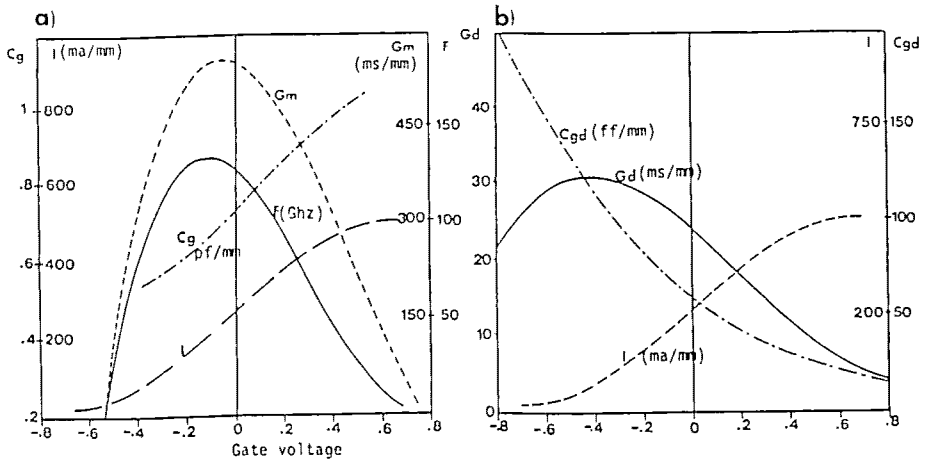

Fig. 4.a) The corresponding small signal parameters evaluated at a drain voltage of 2V a) Transconductance(Gm), gate capacitace (Cgs) and cutoff frequency (Fc). Drain current is also shown. b) Output conductance (Gd) & output capacitance (Cgd).

CONCLUSION

We presented a two-dimensional hydrodynamic energy model that features transient simulations of hot electrons in submicron MODFETs. We introduced two original numerical techniques to take into account deep-level trapping effects and to better incorporate hot electron effects in 2D MOSFET simulators. Further more we suggested a method to treat carrier degeneracy. These methods satisfy the necessity of being accurate and of minor cost.

First obtained results revealed several physical aspects that control carrier transport in MODFETs from which we may cite Parasitic MESFET effects, real space transfer and channel longitudinal field inversion. All of these being related to hot electron effects assessed the importance of the latter in submicron MODFET operation so that simulators that neglect these effects are doubtless.

Development of the physical model to include quantum effects, surface-state effects etc... and of the numérical methods to reduce the computational efforts are important for future research.

REFERENCES

Azoff E.M. (1987). Generalized energy-momentum conservation equations in the relaxation time approximation. Solid state Electronics, 30, 913-917.

El-Sayed O.L. et al (1987). Performance Analysis of sub-Micron Gate GaAs MESFETs. Solid-state Electronics, 30, 643-654.

Ibrahim M. (1983). M.Sc. thesis, Faculty of engineering, Cairo University, Cairo, Egypt.

Loret D. (1987). Two-Dimensional numerical model for the high electron mobility transistor. Solid- State Electronics, 30, 1197-1203.

Lundstron M.S. and Schuelke R.J. (1983). Numerical analysis of heterostructure semiconductor devices. IEEE Trans. ED., 30, 1151-1159.

Marshak A.H. and Van Vlied C. (1984). Electrical current and carrier density in degenerate Materials with nonuniform band structure. Proceedings of the IEEE, 72, 148-164.

Ravaioly U. and Ferry D.K. (1986). MODFET ensemble Monte Carlo Model including the quasi-Two-Dimensional electron gas. IEEE Trans. ED., 33, 677-681.

Shawki T., Salmer G. and El-Sayed O. (1987). Two dimensional transient simulation of submicron-Gate Modfets. Int. Symp. GaAs and Related Compounds, Heraklion, Greece.

Theis T.N. (1987). DX centers in GaAs and AlxGa1-xAs : device instabilities and defect physics. Int. Symp. GaAs and Related compounds, Heraklion, Greece.

Thobel J.L. (1988) Ph.D. Thesis, USTLFA, Lille, France.

Widiger D.J., et al (1985). Two dimensional transient simulation of an idealized High-Electron Mobility Transistor. IEEE Trans. ED., 32, 1092-1102.